Real-Time Visualization of a Focused Ultrasound Beam Using Ultrasonic Backscatter for Monitoring of Mechanical-Based Therapies

Miles Thies and Michael L. Oelze
Department of Electrical and Computer Engineering
Beckman Institute for Advanced Science and Technology
University of Illinois at Urbana-Champaign
Urbana, IL, USA
Email: oelze@illinois.edu

***Abstract*—Mechanical-based focused ultrasound (FUS) therapies use mechanical interactions between an ultrasound wave and tissue to produce localized bioeffects. Although it is a promising therapeutic modality, mechanical-based FUS is limited due to a lack of cost-effective techniques to monitor the FUS beam in real-time during therapy. In this study, we present a technique for the real-time visualization of a FUS beam using ultrasonic backscatter, which could used for the qualitative monitoring of mechanical-based FUS therapies. A diagnostic imaging array was used to transmit a focused visualization pulse and the scattered signal was processed to reconstruct the intensity field of the FUS beam. The imaging array then captured a B-mode image that was registered with the beam reconstruction. The FUS beam reconstruction was superimposed onto the co-aligned B-mode image, allowing one to monitor the location of the FUS beam relative to anatomical information in the B-mode image. The effects of the echogenicity of the medium on the FUS beam reconstruction were reduced using an intensity mask derived from the B-mode image. FUS beam visualizations were demonstrated in a tissue-mimicking phantom and *in vivo* at a frame rate of 25–30 frames per second.**

***Index Terms*—Focused ultrasound, beam visualization, image guidance, mechanical-based therapies**

I. Introduction

Mechanical-based focused ultrasound (FUS) represents a class of non-invasive therapies that has gained the attention of the medical community for its potential in treating many different diseases. Examples include transient opening of the blood brain barrier [1], sensitization of tumors to radiation therapy [2], sonoporation [3], and enhanced bone growth [4]. However, monitoring and guiding the FUS beam in real-time during therapy remains an ongoing problem. Magnetic resonance imaging (MRI) can be used to monitor temperature changes induced by a FUS beam, but the cost and inconvenience associated with MRI are difficult to justify for mechanical-based FUS therapies where temperature elevations in tissue are not necessarily produced. Therefore, there is a need for cost-effective FUS monitoring techniques specific for mechanical-based therapies. Passive cavitation imaging (PCI) is an emerging technique for the monitoring of mechanical-based FUS therapies that visualizes emissions from cavitating microbubbles during therapy [5], [6]. While PCI is a promising method, it has poor axial resolution for therapies where long therapy pulses are used [6] and it requires microbubble injections to visualize cavitation induced by the FUS beam, limiting its use in pre-therapy alignment.

We have developed a novel technique for the monitoring of mechanical-based FUS therapies that uses ultrasonic backscatter from tissue to visualize the FUS beam. This method was previously proposed in [7] where an imaging array was used to passively receive backscatter from a pulse-excited FUS source. The backscatter was then used to reconstruct the intensity field of the FUS beam and the beam reconstruction was overlaid onto a co-aligned B-mode image. In this study, we have expanded on the work in [7] and achieved real-time FUS beam visualizations in non-homogeneous media using a single diagnostic imaging array. To visualize the FUS beam in non-homogeneous media, the co-aligned B-mode image was used to create an intensity mask that equalized the FUS beam reconstruction across local changes in the scattering properties of the medium.

II. Methods

A. Excitation sequence

The excitation sequence used for real-time beam visualization during a FUS therapy is shown in Fig. 1. The FUS beam visualization method requires a FUS source and an imaging array. Two co-aligned transducers can be used or a single diagnostic imaging array can be used as both a FUS source and an imaging array, as was done in this study, if the output levels of the array are sufficient for carrying out therapy. During the off portion of the therapy's duty cycle, the FUS source transmits a focused visualization pulse, which is focused to the same point as the FUS therapy beam. When the visualization pulse is transmitted, the imaging array is triggered to receive the scattered signals. Assuming only single scattering occurs, backscatter will be received only from locations within the FUS beam field and the strength of the scattered signal will

This work was supported by the NIH under Grant R21EB023403.

978-1-7281-5448-0/20/$31.00 ©2020 IEEE

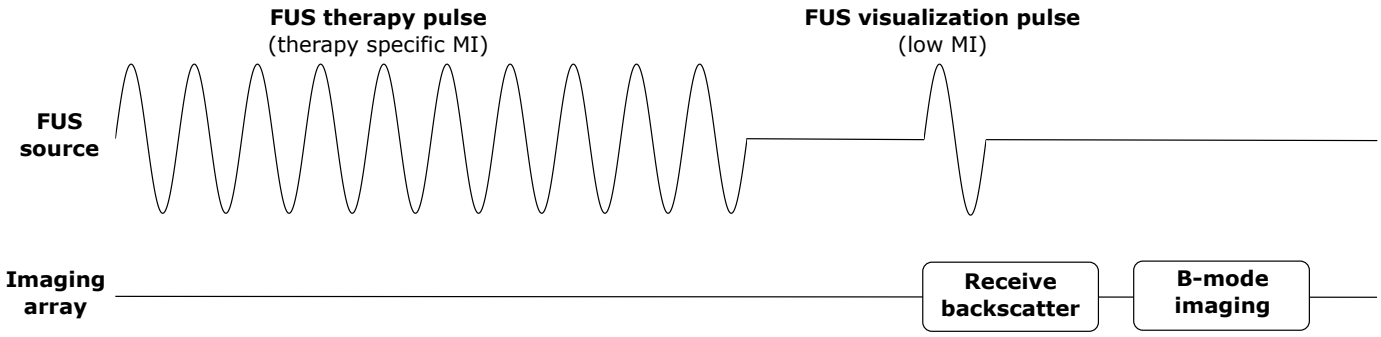

Fig. 1. Excitation sequence for visualization of FUS beam during a mechanical-based FUS therapy.

depend on the local FUS intensity and the scattering properties of the medium. Therefore, the received backscatter can be used to reconstruct the FUS intensity field. A B-mode image is then captured using the imaging array. The FUS beam reconstruction is superimposed onto the co-aligned B-mode image, allowing one to monitor the position of the focused beam relative to the anatomical information in the B-mode image. To minimize any effect that the beam visualization has on the FUS therapy, a low mechanical index (MI) should be used for the focused visualization excitation.

B. FUS beam reconstruction

Delay and sum beamforming with coherence factor (CF) weighting was used to reconstruct the FUS intensity field from the backscattered signal received by the imaging array. The time delays used to focus the imaging array on transmit were included when calculating the beamforming delays. CF weighting is an adaptive beamforming technique that can reduce sidelobes and improve image resolution [8], [9]. The CF is defined as the ratio of the coherent sum to the incoherent sum across the receive aperture and can be expressed as:

$$CF(x,z) = \frac{|\sum_{i=1}^{N} s(x_i,z)|^2}{N\sum_{i=1}^{N}|s(x_i,z)|^2} \tag{1}$$

where $s(x,z)$ is the time delayed RF data for the point (x,z) and N is the size of the receive sub-aperture. CF weighting was necessary to achieve suitable lateral resolution in the FUS beam reconstructions.

The intensity field of the FUS beam was calculated from the beamformed data by using a sliding integral along each scan line. The intensity field $I(x,z)$ at each point can be calculated using:

$$I(x,z) = \sum_{i=0}^{L-1} \Delta z |y(x,z+i)|^2 \tag{2}$$

where $y(x,z)$ is the beamformed data, L is the length of the visualization pulse in samples, and Δz is the axial sampling period.

C. Intensity masking

The backscattered signal received by the imaging array contains information on the location of the FUS beam and the distribution of scatterers in the medium. For the purpose of monitoring mechanical-based therapies, the FUS beam reconstruction should only relay information on the position of the FUS beam because the co-aligned B-mode image already visualizes the distribution of scatterers in the field of view. Thus, an intensity mask was derived from the B-mode image, which was used to equalize the FUS beam reconstruction across areas of different scattering properties. The intensity mask applied a scaling factor $\lambda(x,z)$ to each point in the FUS intensity field, which was calculated using:

$$\lambda(x,z) = 10^{\frac{B_{max}-B(x,z)}{20}} \tag{3}$$

where $B(x,z)$ is the decibel scale B-mode image after being smoothed by passing it through a moving average filter and B_{max} is the maximum value in $B(x,z)$.

The scaling factor $\lambda(x,z)$ was applied to the beamformed data $y(x,z)$ before the pulse intensity integral in equation (2) was computed. The intensity mask was not applied to points where $B(x,z)$ was below -60 dB relative to the maximum because it was assumed signal from these points was largely noise.

D. Experimental configuration

A diagnostic imaging array (Ultrasonix L9-4/38; Center frequency: 5 MHz, Number of elements: 128; Richmond BC, Canada) was driven by a Verasonics Vantage 128 Ultrasound System (Kirkland, WA). The L9-4 array was used as both a FUS source and as an imaging array. The L9-4 array can produce peak negative pressure values up to 2.4 MPa as measured using a needle hydrophone in degassed water, which is above the pressure values needed for many mechanical-based FUS therapies. Data were collected from a tissue-mimicking phantom (Supertech ATS 539; Elkhart, IN) and a rat tumor *in vivo*. The excitation sequence began with a 25 cycle focused pulse at 5 MHz to simulate a FUS therapy beam. Next, the L9-4 array transmitted and received backscatter from a 2 cycle focused visualization pulse at 5 MHz, which was focused to the same location as the mock FUS therapy beam.

The L9-4 array then transmitted and received a series of seven steered plane waves ($-18°$ to $18°$) for the formation of a B-mode image using coherent plane wave compounding [10]. The FUS beam reconstruction algorithm was implemented on a GPU (NVIDIA Quadro P2000; Santa Clara, CA) and the B-mode image was formed using the built-in Verasonics beamformer. The focused visualization pulse had a MI of 0.54 as measured using a needle hyrdophone in degassed water.

E. Animal experiment

The protocol was approved by the Institutional Animal Care and Use Committee (IACUC) at the University of Illinois at Urbana-Champaign. MAT tumor cells (100 μL containing $5 \times 10^2 - 1 \times 10^5$ cells) were injected into the mammary fat pad of a rat. After the tumor had grown to more than 1 cm in diameter, the animal was anesthetized with isoflurane and scanned using the FUS beam visualization technique. The posterior half of the animal was submerged in degassed water at 37 °C to allow a standoff distance of 1–2 cm while scanning.

III. Results

A FUS beam reconstruction was demonstrated in a tissue-mimicking phantom (Fig. 2). The FUS beam reconstruction that is displayed includes the application of the intensity mask. The FUS beam can be clearly visualized in the context of the surrounding medium. The phantom contained circular anechoic regions. As expected, the FUS beam was not reconstructed within these anechoic regions because no signal was scattered back to the imaging array, although noise is still present in these regions.

FUS beam visualizations were demonstrated in a rat tumor *in vivo* (Fig. 3). In Fig. 3a, a FUS beam reconstruction is shown before applying the intensity mask calculated from the B-mode image. The position and extent of the FUS beam are difficult to identify because only a small amount of backscattered signal was received from the hypoechoic tumor and the FUS intensity field within the tumor was below the dynamic range used for display. After the intensity mask was applied in Fig. 3b, the FUS beam could be clearly visualized because parts of the FUS beam reconstruction that corresponded to weakly scattering regions in the co-aligned B-mode image were amplified. A frame rate of 25–30 frames per second was achieved while visualizing the FUS beam and surrounding tissue.

IV. Discussion

In this study, a technique for the real-time visualization of a FUS beam using ultrasonic backscatter has been presented. A single diagnostic imaging array was used to transmit and visualize a FUS beam. FUS beam reconstructions were demonstrated in non-homogeneous media using a process we call intensity masking where a mask is derived from the co-aligned B-mode image that amplifies regions of weak scattering. Real-time FUS beam reconstructions were achieved in a tissue-mimicking phantom and *in vivo*.

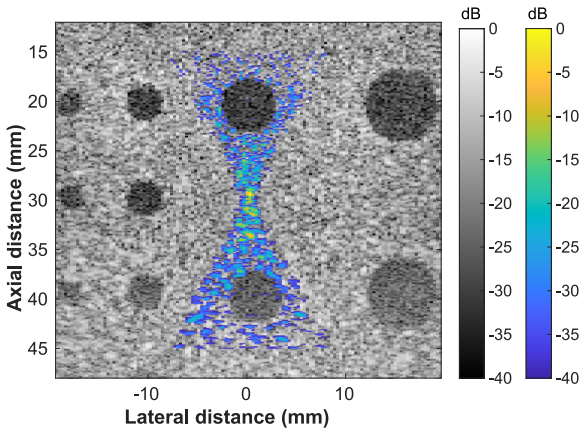

Fig. 2. FUS beam reconstruction (blue/yellow) overlaid onto B-mode image (grayscale) captured from a tissue-mimicking phantom. The FUS beam was targeted to 30 mm using all 128 elements of the L9-4 array.

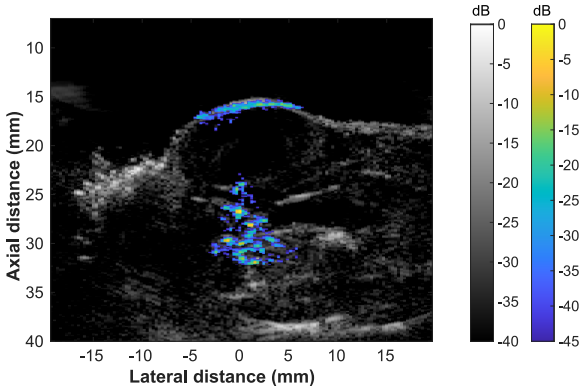

(a)

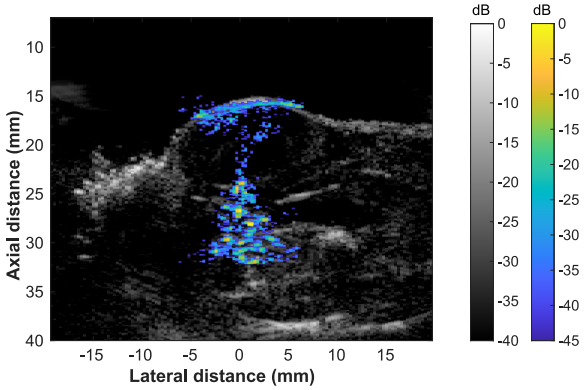

(b)

Fig. 3. FUS beam reconstructions captured from a rat tumor *in vivo*. The FUS beam was targeted to 22 mm using all 128 elements of the L9-4 array. (a) Before intensity masking. (b) After intensity masking.

The main benefit of this technique over other FUS monitoring methods is its simplicity. A FUS beam can be visualized using a single diagnostic imaging array without microbubbles. Two co-registered transducers operating at similar frequencies can also be used assuming the FUS source can transmit short duration excitations because the axial resolution of the FUS beam reconstruction depends on the length of the focused

visualization pulse. Considering the similarities between this method and conventional B-mode imaging, many techniques that have been developed to improve the spatial or temporal resolution of B-mode imaging could also be applied to this method. For example, CF weighting was successful in improving lateral resolution of the FUS beam reconstructions in this study.

Monitoring of a FUS beam using ultrasonic backscatter visualizes interactions between the FUS beam and tissue at the fundamental frequency. PCI differs from this method in that PCI visualizes interactions between the FUS beam and microbubbles at harmonics of the fundamental frequency. PCI relies on mechanical phenomenon induced by the FUS therapy beam, meaning the imaging capabilities of PCI depend on the type of mechanical-based FUS therapy being carried out. Using our method, the FUS beam visualization is done independently of the FUS therapy. While this is beneficial in many ways, one limitation that has not yet been explored is that the FUS visualization beam could interfere with the mechanical-based FUS therapy. Interactions between the FUS visualization beam and tissue or microbubbles can be minimized by using a low MI for the FUS visualization pulse. However, lowering the MI will decrease the signal-to-noise ratio of the FUS beam reconstruction.

Another key difference is that PCI can provide quantitative information on cavitation activity that is correlated with bioeffects during therapy. Our method was only used for qualitative monitoring of the position of the FUS beam. In [7], spatial compounding was used to make quantitative measurements of FUS beam properties, but compounding was not discussed in this study because real-time qualitative monitoring was the main goal. For mechanical-based FUS therapies where quantitative monitoring is required, our method could still be used for pre-therapy alignment and real-time visualization of the FUS beam at the fundamental frequency.

Real-time FUS beam visualization using ultrasonic backscatter could provide a cost-effective and simple technique for pre-therapy alignment and monitoring of mechanical-based FUS therapies. This method could be used to monitor the position and range of a FUS beam during therapy to ensure that the beam is continuously targeted to the correct region in the presence of tissue motion.

REFERENCES

[1] A. Carpentier, M. Canney, A. Vignot, V. Reina, K. Beccaria, C. Horodyckid, C. Karachi, D. Leclercq, C. Lafon, J.-Y. Chapelon, L. Capelle, P. Cornu, M. Sanson, K. Hoang-Xuan, J.-Y. Delattre, and A. Idbaih, "Clinical trial of blood-brain barrier disruption by pulsed ultrasound," *Sci. Transl. Med.*, vol. 8, no. 343, pp. 343re2–343re2, Jun. 2016.

[2] J. R. Eisenbrey, R. Shraim, J.-B. Liu, J. Li, M. Stanczak, B. Oeffinger, D. B. Leeper, S. W. Keith, L. J. Jablonowski, F. Forsberg, P. O'Kane, and M. A. Wheatley, "Sensitization of hypoxic tumors to radiation therapy using ultrasound-sensitive oxygen microbubbles," *Int. J. Radiat. Oncol. Biol. Phys.*, vol. 101, no. 1, pp. 88–96, 2018.

[3] I. Lentacker, I. De Cock, R. Deckers, S. De Smedt, and C. Moonen, "Understanding ultrasound induced sonoporation: definitions and underlying mechanisms," *Adv. Drug Deliv. Rev*, vol. 72, pp. 49–64, 2014.

[4] Y. J. Jung, R. Kim, H.-J. Ham, S. I. Park, M. Y. Lee, J. Kim, J. Hwang, M.-S. Park, S.-S. Yoo, L.-S. Maeng *et al.*, "Focused low-intensity pulsed ultrasound enhances bone regeneration in rat calvarial bone defect through enhancement of cell proliferation," *Ultrasound Med. Biol*, vol. 41, no. 4, pp. 999–1007, 2015.

[5] M. Gyöngy and C.-C. Coussios, "Passive spatial mapping of inertial cavitation during hifu exposure," *IEEE Trans. Biomed. Eng.*, vol. 57, no. 1, pp. 48–56, 2009.

[6] K. J. Haworth, K. B. Bader, K. T. Rich, C. K. Holland, and T. D. Mast, "Quantitative frequency-domain passive cavitation imaging," *IEEE Trans. Ultrason., Ferroelectr., Freq. Control*, vol. 64, no. 1, pp. 177–191, Jan. 2017.

[7] T. N. Nguyen, M. N. Do, and M. L. Oelze, "Visualization of the intensity field of a focused ultrasound source in situ," *IEEE Trans. Med. Imaging*, vol. 38, no. 1, pp. 124–133, Jan. 2019.

[8] R. Mallart and M. Fink, "Adaptive focusing in scattering media through sound-speed inhomogeneities: The van Cittert Zernike approach and focusing criterion," *J. Acoust. Soc. Am.*, vol. 96, no. 6, pp. 3721–3732, Dec. 1994.

[9] K. Hollman, K. Rigby, and M. O'donnell, "Coherence factor of speckle from a multi-row probe," in *1999 IEEE Int. Ultrason. Symp. (Cat. No. 99CH37027)*, vol. 2. IEEE, 1999, pp. 1257–1260.

[10] G. Montaldo, M. Tanter, J. Bercoff, N. Benech, and M. Fink, "Coherent plane-wave compounding for very high frame rate ultrasonography and transient elastography," *IEEE Trans. Ultrason., Ferroelectr., Freq. Control*, vol. 56, no. 3, pp. 489–506, 2009.